Heriot-Watt University
Research Gateway

Simultaneous Design and Integration of Multiple Processes for Eco-Industrial Park Development

Citation for published version:
Foong, SZY & Ng, DKS 2021, 'Simultaneous Design and Integration of Multiple Processes for Eco-Industrial Park Development', *Journal of Cleaner Production*, vol. 298, 126797.
https://doi.org/10.1016/j.jclepro.2021.126797

Digital Object Identifier (DOI):
10.1016/j.jclepro.2021.126797

Link:
Link to publication record in Heriot-Watt Research Portal

Document Version:
Peer reviewed version

Published In:
Journal of Cleaner Production

Publisher Rights Statement:
© 2021 Elsevier Ltd.

General rights
Copyright for the publications made accessible via Heriot-Watt Research Portal is retained by the author(s) and / or other copyright owners and it is a condition of accessing these publications that users recognise and abide by the legal requirements associated with these rights.

Take down policy
Heriot-Watt University has made every reasonable effort to ensure that the content in Heriot-Watt Research Portal complies with UK legislation. If you believe that the public display of this file breaches copyright please contact open.access@hw.ac.uk providing details, and we will remove access to the work immediately and investigate your claim.

Download date: 22. Apr. 2025

Simultaneous Design and Integration of Multiple Processes for Eco-Industrial Park Development

Steve Z. Y. Foong [a,b], *Denny K. S. Ng* [b,*]

[a] *Department of Chemical and Environmental Engineering, University of Nottingham Malaysia, Broga Road, Semenyih 43500, Malaysia*

[b] *School of Engineering and Physical Sciences, Heriot-Watt University Malaysia, 62200, Putrajaya, Wilayah Persekutuan Putrajaya, Malaysia*

Abstract

Process integration techniques have been established in various areas, which include energy recovery, in-plant material recovery, industrial symbiosis, energy planning, financial management, etc. Such techniques are well accepted in the research community and industrial applications. Synthesising and designing an eco-industrial park via process integration techniques is recognised as one of the most effective strategies to promote sustainable industrial systems. Feasible operating range analysis has been introduced to evaluate and determine the true operating potential of an eco-industrial park coalition without experiencing design and performance limitations. Such tool also acts as a comprehensive decision-making tool for designers to evaluate the performance of an integrated process at different operational states. In this perspective, a novel mixed-integer linear programming model is presented in this work for simultaneous design and integration of multiple processes to form an eco-industrial park. The true potential and performance of the eco-industrial park developed are assessed at different operational states. To illustrate the proposed approach, an industrial case study on

[*] Denny K. S. Ng (Email: denny.ng@hw.ac.uk, Tel: +603 8894 3784)

design of eco-industrial park in oil palm industry, which consists of palm oil mill, integrated biogas and wastewater treatment system, palm-based biorefinery, and combined heat and power system, is solved and presented.

Keywords: *Feasible operating range analysis; Simultaneous design and integration; Process systems engineering; Industrial symbiosis; Eco-industrial park in oil palm industry***.**

1. Introduction

"Industrial ecology" is traditionally used to evaluate the flows of material and energy within industrial systems (i.e., industrial metabolism). The principal objective of industrial ecology is to translate the conventional linear systems into a closed-loop system to enhance the overall efficiency of integrated systems (Lowe and Evans, 1995; Ehrenfeld and Gertler, 1997). Later, the concept of industrial symbiosis (IS), also known as an eco-industrial park (EIP), was introduced and emerged to allow the exchange of resources between systems in a mutually beneficial manner to strive for more mutual benefits and sustainability in the industry (Chertow, 2000). In that case, materials, including by-products/waste, are interchangeable and utilised to substitute commercial products or raw materials in another system. Besides, resources such as energy and utility water can also be shared within EIP, while service provisions for ancillary activities such as fire suppression, transportation, and food provision may be combined to fulfil everyday needs across firms (Chertow, 2007; Chertow et al., 2008). Such interactions increase the overall efficiency of resources used, reduce emissions, and eliminate wastes, as compared to the plant which operates independently.

Over the years, numerous systematic process integration (PI) tools have been developed to facilitate the design of efficient and sustainable EIP coalitions. For instance, Bandyopadhyay et al. (2010) proposed an insight-based pinch analysis approach to estimate the cogeneration

potential at total site level for simultaneous heat and power targeting among multiple processes. The similar approach is adapted and improved to design a total site heat exchanger network with multiple steam qualities for maximum heat recovery (Liew et al., 2013, 2014). Such an approach is proven effective in solving large-scale interplant heat integration network (Song et al., 2017a, 2017b). Besides utility network synthesis, pinch analysis has also been applied for interplant hydrogen network with direct and purification reuse/recycling schemes (Deng et al., 2015), as well water networks for minimum freshwater requirement and wastewater generation (Fadzil et al., 2017). Recently, Kamat and Bandyopadhyay (2019) developed a systematic framework to synthesise both heat exchanger and water networks simultaneously using pinch analysis in EIPs.

Apart from pinch analysis, mathematical programming approaches have also been developed for the synthesis of sustainable EIP. Chew and co-workers (2008; 2009) formulated linear programming (LP) and mixed-integer linear programming (MILP) models to minimise freshwater and wastewater flowrates in multiple processing plants with a centralised utility hub. A bi-level fuzzy optimisation model is then proposed by Aviso et al. (2010) to determine the optimal interplant water integration networks with minimum freshwater consumption while considering individual financial goals in an EIP. The work is further extended to include water regeneration and redistribution through a centralised hub (Tan et al., 2011). Since then, various mathematical models ranging from LP to non-linear programming (NLP) have been developed to synthesise interplant utility networks such as heat exchanger network (Chae et al., 2010; Bade and Bandyopadhyay, 2014), water network (Rubio-Castro et al., 2010, 2012; Jiang et al., 2019) integrated heat and water network (Lee et al., 2014), integrated carbon, hydrogen, and oxygen symbiosis network (Noureldin and El-Halwagi, 2015; El-Halwagi, 2017), chilled and cooling water network (Leong et al., 2016), algae-based EIP (Ubando et al., 2016), and hydrogen network (Deng et al., 2017).

For instance, Ng and Ng (2013) have formulated an MILP model to promote integration among different processing plants and recovery of by-products to establish a conceptual integrated palm oil processing complex (POPC). The developed model allows for a systematic approach in synthesing and optimising a POPC to achieve maximum economic performance for single owner. Satisfactory level in terms of economic interests (Ng et al., 2013b), environment, and inherent safety (Ng et al., 2014) are then considered to address the individual interests of different owners in the POPC coalition. A novel disjunctive fuzzy optimisation approach is proposed by Ng and coworkers (2014) to determine the optimum pathways based on processing plants' declared interests in an oil palm-based EIP (OPEIP). Andiappan et al. (2016) also presented a negotiation framework based on game theory and LP model to allocate fair benefits among various processes for an oil palm-based EIP case study.

While extensive research works have been performed in developing the EIP coalition using PI tools (pinch analysis and mathematical optimisation approaches), it is noted that all the previous studies assumed a steady-state operation to ease the optimisation process. Limited attention has been paid to the operability of individual systems within the entire EIP coalition. According to Grossmann and Morari (1983), the term 'operability' is defined as the ability to perform satisfactorily under conditions apart from the nominal design conditions. In the industry, most processes are often built with an excess capacity, based on the engineers' experience to ensure higher flexibility for a broader range of operating conditions (Kittrell and Watson, 1966; Sharifzadeh, 2013) and lower processing costs (i.e., labour, service, and maintenance costs) (Azman, 2014). Nevertheless, such an over-design can be expensive and impractical sometimes to handle the actual process needs (Lai and Hui, 2009). The impact of oversizing is observed during the lean production seasons when the utilisation or economic performance falls out of the feasible range designated. In this respect, Ng and his co-workers (Andiappan et al., 2017) proposed a novel feasible operating range analysis (FORA) to examine

99 the real-time feasible operating range of a process in graphical means. The methodology of
100 FORA was adopted from Lai and Hui (2009), in which the feasibility and flexibility of a pre-
101 designed process were determined. Besides, Foong et al. (2019) performed FORA to study the
102 utilisation and flexibility of the developed design of a palm oil mill.

103 Note that FORA allows the operational performance of a system designed to be
104 measured using utilisation (*UI*) and flexibility indexes (*FI*). The former is defined as the ratio
105 of capacity utilised (Siddiqi and Glass, 1981; Malakrong et al., 2017), while the latter
106 represents a weighted ratio that compares the likelihood of a process to alter from the defined
107 specification (Grossmann et al., 1983; Kazmer et al., 2003). Such an approach can be extended
108 to determine the true process bottlenecks (Kasivisvanathan et al., 2014; Tan et al., 2012).
109 Process bottleneck occurs when a processing unit reaches its capacity limit, typically, during
110 yield alterations, throughput increment, input or raw materials limitation, specification
111 modifications, or more stringent emission limits (Schneider, 1997). Depending on the nature
112 of bottleneck identified, various debottlenecking strategies such as operating conditions
113 adjustment, process intensification (Ponce-Ortega et al., 2012; Enríquez-Gutiérrez et al., 2015),
114 and adding new equipment units (Kasivisvanathan et al., 2014) can be implemented to meet
115 the new constraints. In that respect, FORA enables process designers to recognise the true
116 operating potential before identifying possible debottlenecking approach systematically based
117 on the benefit-cost ratio (Kasivisvanathan et al., 2014). For instance, Andiappan et al. (2017)
118 presented the operational performance and debottlenecking strategies for a biomass-based tri-
119 generation system during various energy production levels. Apart from that, Foong et al. (2019)
120 also performed an analysis on a real-time feasible operating range to determine the bottleneck
121 for palm oil mill (POM) of different design capacities.

122 As shown in the literature, PI techniques range from simplistic LP to more complicated
123 MINLP models were proven effective in conceptualising EIP coalitions. Meanwhile, FORA

124 can be applied to study the operation of a process designed and serves as a decision-making
125 tool under distinct operational states. However, none of the recent and relevant studies focused
126 on developing an integrated system consisting of multiple processes with consideration of
127 feasible operating range simultaneously. In this regard, a general MILP model is proposed in
128 this work for simultaneous grassroot design of individual processes and interplant integrations,
129 followed by FORA to consider the real operations of the EIP coalition established. Such a
130 coalition focuses on the physical exchanges of materials, energy, water, and by-products while
131 considering the capacity constraints among processes to develop a symbiotic and recycling
132 network within the industry. The objective is to evaluate the incremental in both economic and
133 environmental gains concerning the additional capital investments needed to establish such a
134 coalition as compared to individual operations. Besides, FORA allows the global feasible (GF)
135 operation and bottlenecking process within the EIP coalition formed be determined. The
136 developed MILP model is formulated in a commercial software LINGO (version 16.0) with
137 Global solver (LINDO Systems Inc., 2017).

138 The rest of the paper is organised as follows. The problem addressed is first described
139 in Section 2, followed by the methodology used for developing the mathematical model. An
140 oil palm processing case study is solved and presented in Section 4 to illustrate the developed
141 model. Section 5 then discussed the results, key findings, and operational analysis of the case
142 study. Lastly, conclusions and prospects for future work are given in Section 6.

143

144 ## 2. Problem Statement

145 The problem addressed by the proposed approach is stated as follows. A given set of
146 process $p \in P$ from the same site is interested in forming an EIP coalition. Process p consists of
147 a set of technologies $te \in TE$ with interchangeable materials $m \in M$. The input and output matrix

of process p is given as $\mathbf{A}_{m,te,p}$, where the output of material m from process p may be utilised as input in another process p.

The existence of process p is denoted by the set binary variables $\mathbf{B}_{p,}$ and each process p consists of a set of maximum equipment units for technology te installed, $\mathbf{U}_{te,p}^{\max}$ with the nominal capacity, $\mathbf{CAP}_{te,p}$. In this work, the objective is to derive a systematic approach to develop an optimal EIP coalition, which yields maximum economic performance, EP_{EIP}, as shown in Eq. 1. Following this, FORA is performed to measure the operability of individual process p and the entire coalition formed, identifying the global feasible operating range and bottlenecking process within the alliance. The changes in EP_p and EP_{EIP} are predicted based on the input and output of material m in process p ($y_{m,p}$), and the coalition formed ($y_{m,\text{IS}}$).

$$\text{Maximise } EP_{\text{EIP}} \tag{1}$$

3. Model Formulation

In this section, the mathematical model presented considers multiple processes p where the exchange of material m between processes p is allowed to form an integrated EIP coalition. Note that variables and fixed parameters are represented by italic and non-italic mathematical notations, respectively, while bold notations signify matrix or vector symbols.

A linear correlation of material m in technology te across process p is assumed as given in Eq. 2

$$\mathbf{B}_p \mathbf{A}_{m,te,p} \boldsymbol{x}_{te,p} = \boldsymbol{y}_{m,p} \qquad \forall m, p \tag{2}$$

where $\mathbf{B}_p$, $\mathbf{A}_{m,te,p}$, $\boldsymbol{x}_{te,p}$, and $\boldsymbol{y}_{m,p}$ are the set of binary parameters denoting the existence of process p, the matrix of fixed interaction ratios between material m and technology te, throughput vector of technology te, and flowrate vector of material m in process p, respectively. The presence of process p is specified as one by $\mathbf{B}_p$ and zero in the absence of it. Meanwhile, $\mathbf{A}_{m,te,p}$

is expressed as negative value as input, while positive value as output of material *m* in technology *te* in process *p*. In the event where no interaction is occurring between material *m* in technology *te* in process *p*, $\mathbf{A}_{m,te,p}$ will be expressed as zero. A positive value in $\boldsymbol{x}_{te,p}$ represents the throughput of technology *te* operated in process *p*. On the other hand, $\boldsymbol{x}_{te,p}$ is shown as zero when the particular technology *te* in process *p* is not operated. $\boldsymbol{y}_{m,p}$ expresses the feedstock, intermediate, and product of process *p* in a negative value, zero, and positive value, respectively. Note that both $\boldsymbol{x}_{te,p}$ and $\boldsymbol{y}_{m,p}$ are expressed in material flow rate (e.g., kt/y) or power generation (e.g., MWh). The summation of $\boldsymbol{y}_{m,p}$ gives the flowrate vector of material *m* for the overall EIP coalition ($\boldsymbol{y}_{m,\mathrm{EIP}}$), as shown in Eq. 3.

$$\boldsymbol{y}_{m,\mathrm{EIP}} = \sum_{p=1}^{\mathrm{P}} \boldsymbol{y}_{m,p} \qquad \forall m \qquad (3)$$

The vector for the units of technology *te* operated in process *p* ($\boldsymbol{U}_{te,p}$) can be obtained via Eq. 4

$$\boldsymbol{U}_{te,p} \geq \boldsymbol{x}_{te,p} \left(\mathbf{CAP}_{te,p}\right)^{-1} \qquad \forall te, p \qquad (4)$$

where $\mathbf{CAP}_{te,p}$ is the diagonal matrix for a nominal capacity of technology in process *p*, found in the market. $\boldsymbol{U}_{te,p}$ consists of positive integers when technology *te* is operated in process *p*. Otherwise, it appears as zero when $\boldsymbol{x}_{te,p}$ is zero. In order to ensure that $\boldsymbol{U}_{te,p}$ does not exceed the maximum units of technology *te* installed for process *p* ($\mathbf{U}_{te,p}^{\max}$),Eq. 5 is added as a constraint to the mathematical model.

$$\mathbf{U}_{te,p}^{\max} \geq \boldsymbol{U}_{te,p} \qquad \forall te, p \qquad (5)$$

In this model, the electricity demand of process *p* ($E_{e,p}^{\mathrm{Demand}}$) is determined based on $\boldsymbol{U}_{te,p}$ as shown in Eq. 6

$$E_{e,p}^{\mathrm{Demand}} = \sum_{te=1}^{\mathrm{TE}} \boldsymbol{U}_{te,p} \mathbf{E}_{te,p} \qquad \forall te, p \qquad (6)$$

where $\mathbf{E}_{te,p}$ is the diagonal matrix for electricity consumption specified per unit technology *te* operated in process *p*. The total electricity demand of the EIP coalition formed, $E_{e,\mathrm{EIP}}^{\mathrm{Demand}}$ can be determined via Eq. 7.

$$E_{e,\mathrm{EIP}}^{\mathrm{Demand}} = \sum_{p=1}^{\mathrm{P}} E_{e,p}^{\mathrm{Demand}} \tag{7}$$

For conservative measurement, the power consumption and process efficiency for maximum loading are assumed for each operating equipment to prevent underestimation of power demand needed, regardless of the process throughput for each machine. Every technology unit *te* is sized based on these conservative values to ensure the developed system's reliability. As such, whenever a piece of equipment is selected, a conservative electricity consumption value (or maximum) is activated and determined.

The economic performance of the EIP coalition formed, EP_{EIP} is given as the summation of economic performance for process *p* (EP_p), which is obtained from the gross profit, GP_p, capital recovery factor, CRF, and capital costs required, CAPEX_p of process *p*.

$$EP_{\mathrm{EIP}} = \sum_{p=1}^{\mathrm{P}} EP_p \tag{8}$$

$$EP_p = GP_p - \mathrm{CRF} \times \mathrm{CAPEX}_p \qquad \forall p \tag{9}$$

Note that both EP_{EIP} and EP_p must be greater or equal to zero to ensure the economic feasibility of the developed EIP coalition and individual process *p*. In the event that EP_{EIP} and EP_p have the negative value, the EIP and respective process *p* is not economically feasible. Eq. 10 shows GP_p of individual process *p*.

$$GP_p = \sum_{m=1}^{\mathrm{M}} \boldsymbol{y}_{m,p} \mathbf{C}_m - E_{e,p}^{\mathrm{Demand}} \mathrm{C}_e^{\mathrm{Imp}} - OPEX_p - \mathrm{LC}_p \qquad \forall p \tag{10}$$

whereby $\mathbf{C}_m$, $\mathrm{C}_e^{\mathrm{Imp}}$, $OPEX_p$, and LC_p are the costs of material *m*, cost of electricity imported, total operating expenses, and labour costs for process *p*, respectively. In the model, it is

assumed that all electricity generated by process p, $y_{e,p}$ is sold to the national grid. Meanwhile, $E_{e,p}^{\text{Demand}}$ to operate process p will be purchased from the national grid.

In order to annalise the CAPEX_p , CRF is introduced in the mathematical model based on the operation lifespan, $\text{t}_{te}^{\max}$ and discount rate, r, as shown in Eq. 11.

$$\text{CRF}=\frac{\text{r}\,(1+\text{r})^{\text{t}_{te}^{\max}}}{(1+\text{r})^{\text{t}_{te}^{\max}}-1} \tag{11}$$

Meanwhile, CAPEX_p can be determined via Eq. 12

$$\text{CAPEX}_p=\sum_{te=1}^{\text{TE}}\mathbf{U}_{te,p}^{\max}\mathbf{CC}_{te,p} \qquad \forall p \tag{12}$$

where $\mathbf{CC}_{te,p}$ is the diagonal matrix of capital costs per unit of technology te in process p. On the other hand, Eq. 13 can be used to determined the $OPEX_p$

$$OPEX_p=\sum_{te=1}^{\text{TE}}\boldsymbol{U}_{te,p}\mathbf{OC}_{te,p} \qquad \forall p \tag{13}$$

where $\mathbf{OC}_{te,p}$ is the diagonal matrix of operating costs per unit of technology te in process p. The summation of CAPEX_p and $OPEX_p$ gives the total capital costs, $\text{CAPEX}_{\text{EIP}}$ and operating costs, $OPEX_{\text{EIP}}$ of the EIP coalition formed, respectively.

$$\text{CAPEX}_{\text{EIP}}=\sum_{p=1}^{\text{P}}\mathbf{B}_p\text{CAPEX}_p \tag{14}$$

$$OPEX_{\text{EIP}}=\sum_{p=1}^{\text{P}}OPEX_p \tag{15}$$

LC_p is determined based on the number of workers in process p, $\text{n}_{\text{wk},p}$ and a fixed costs of labour, C_{lab} specified, given in Eq. 16.

$$\text{LC}_p=\text{n}_{\text{wk},p}\text{C}_{\text{lab}} \qquad \forall p \tag{16}$$

The summation of greenhouse gas (GHG) emissions from process *p*, GHG_p gives the total GHG emissions from the EIP coalition developed, GHG_{EIP}, as shown in Eq. 17. GHG_p is evaluated based on Eq. 18

$$GHG_{\mathrm{EIP}} = \sum_{p=1}^{\mathrm{P}} GHG_p \tag{17}$$

$$GHG_p = \sum_{m=1}^{\mathrm{M}} \boldsymbol{y}_{m,p}\, \mathbf{SER}_m \qquad \forall p \tag{18}$$

where $\mathbf{SER}_m$ is the specific emissions rate for material *m*. $\mathbf{SER}_m$ is assigned with a positive value when GHG is emitted during the production or disposal of material *m*, and vice versa. Meanwhile, $\mathbf{SER}_m$ is specified as zero for carbon-neutral materials.

FORA is then performed to identify the GF operating range of the EIP coalition designed. The analysis begins by optimising the objective function given in Eq. 1 with an assumption that an infinite amount of input material *m* available. Based on the $\mathbf{U}_{te,p}^{\max}$ specified, both $\boldsymbol{y}_{m,p}$ and $\boldsymbol{y}_{m,\mathrm{EIP}}$ will be capped at a maximum value of $\boldsymbol{y}_{m,p}^{\max}$ and $\boldsymbol{y}_{m,\mathrm{EIP}}^{\max}$, respectively. In that respect, the maximum *EP* achievable by each process *p*, $EP_p^{\max}$ and the entire coalition, $EP_{\mathrm{EIP}}^{\max}$ can be determined based on Eqs. 8 and 9. Next, the model is resolved with an additional constraint given in Eq. 19 to identify the minimum value of $\boldsymbol{y}_{m,p}$ ($\boldsymbol{y}_{m,p}^{\min}$) while ensuring the operation for process *p* is economically stable to sustain by itself.

$$EP_p = 0 \qquad \forall p \tag{19}$$

Following that, the minimum value of $\boldsymbol{y}_{m,\mathrm{EIP}}$ ($\boldsymbol{y}_{m,\mathrm{EIP}}^{\min}$) is identified by modifying the constraint in Eq. 19 into Eq. 20.

$$EP_{\mathrm{EIP}} = 0 \tag{20}$$

For any given y_m, the economic potential index for process p, EPI_p and the EIP coalition developed, EPI_{EIP} are calculated using Eqs. 21 and 22 to determine the fraction of EP_p and EP_{EIP} over $EP_p^{\max}$ and $EP_{\mathrm{EIP}}^{\max}$, respectively.

$$EPI_p = EP_p \big/ EP_p^{\max} \qquad \forall p \qquad (21)$$

$$EPI_{\mathrm{EIP}} = EP_{\mathrm{EIP}} \big/ EP_{\mathrm{EIP}}^{\max} \qquad (22)$$

Both EPI_p and EPI_{EIP} range between zero to one where zero indicates that the process p and EIP coalition are not making any profit or loss. Meanwhile, EPI_p and EPI_{EIP} are reported as one when the highest EP is achieved for process p and the EIP coalition, respectively.

Apart from that, the utilisation index, UI and flexibility index, FI are introduced in this work to measure the operability of each process p and the alliance formed in Eqs. 23 – 26

$$UI_p = y_{m,p} \big/ y_{m,p}^{\max} \qquad \forall p \qquad (23)$$

$$UI_{\mathrm{EIP}} = y_{m,\mathrm{EIP}} \big/ y_{m,\mathrm{EIP}}^{\max} \qquad (24)$$

$$FI_p = \begin{cases} FI_p^{\mathrm{U}} = (y_{m,p}^{\max} - y_{m,p}) \big/ y_{m,p}^{\max} \\ FI_p^{\mathrm{L}} = (y_{m,p} - y_{m,p}^{\min}) \big/ y_{m,p}^{\max} \end{cases} \qquad \forall p \qquad (25)$$

$$FI_{\mathrm{EIP}} = \begin{cases} FI_{\mathrm{EIP}}^{\mathrm{U}} = (y_{m,\mathrm{EIP}}^{\max} - y_{m,\mathrm{EIP}}) \big/ y_{m,\mathrm{EIP}}^{\max} \\ FI_{\mathrm{EIP}}^{\mathrm{L}} = (y_{m,\mathrm{EIP}} - y_{m,\mathrm{EIP}}^{\min}) \big/ y_{m,\mathrm{EIP}}^{\max} \end{cases} \qquad (26)$$

where UI_p, UI_{EIP}, FI_p^{U}, $FI_{\mathrm{EIP}}^{\mathrm{U}}$, FI_p^{L}, and $FI_{\mathrm{EIP}}^{\mathrm{L}}$ are the utilisation, upper and lower flexibility index of process p and EIP coalition established, respectively. Note that the flowrate of a crucial material m, usually the raw material or final product represents the entire flowrate vector of material m ($\boldsymbol{y}_m$). Both UI and FI range from zero to one. In the event where UI_p equals zero, the process p is not operated, while one indicates that it is running at 100% of its processing capacity installed (Malakrong et al., 2017). Meanwhile, zero in FI_p^{U} and FI_p^{L} represent that process p is not capable of tolerating any increment and decrement, respectively, in y_m without

interrupting the operation, and vice versa. That is to say, when UI_p and FI_p^{U} equal to 1 and 0, respectively, $y_{m,p}$ will be capped at $y_{m,p}^{\max}$ with no further increment in product generated. On the other hand, $y_{m,p}$ approaches $y_{m,p}^{\min}$ when UI_p and FI_p^{L} equal to 1 and 0, resulting in a negative profit if $y_{m,p}$ is reduced further. The same principle is also applied for UI_{EIP}, FI_p^{L}, and $FI_{\mathrm{EIP}}^{\mathrm{L}}$ in the EIP coalition established.

For a better illustration of the proposed FORA, a graphical representation for a simple coalition between two processes is given in **Figure 1**. Several key features to be highlighted from the analysis are as follows. $y_{m,\mathrm{EIP}}^{\max}$ and $y_{m,\mathrm{EIP}}^{\min}$ are represented by dotted lines in **Figure 1 (a)** with the range of y_m between these two lines is labelled as the feasible (FE) range, shaded in orange colour. Beyond this range ($y_m > y_{m,\mathrm{EIP}}^{\max}$), the costs needed to operate the additional throughput outweighs the profit generated, reducing the EP_{EIP} obtained. Meanwhile, when y_m falls below $y_{m,\mathrm{EIP}}^{\min}$, the coalition formed is economically infeasible as negative EP_{EIP} is attained. These regions are labelled as the not feasible (NF) range and shaded in red. The arrows represent the feasible operating range of each process p, where $y_{m,p}^{\max}$ and $y_{m,p}^{\min}$ are shown by the upper and lower arrows, respectively. In this example, the blue arrow shows the feasible operating range of process 1, while the orange arrow indicates the feasible operating range of process 2. Occasionally, $y_{m,p}^{\max}$ and $y_{m,p}^{\min}$ may fall out of the FE region (within the NF region) when $y_{m,p}^{\max}$ exceeds $y_{m,\mathrm{EIP}}^{\max}$ or $y_{m,p}^{\min}$ is lower than $y_{m,\mathrm{EIP}}^{\min}$. For instance, the maximum throughput in process 2 is higher than the developed alliance ($y_{m,2}^{\max} > y_{m,\mathrm{EIP}}^{\max}$). This indicates that y_m higher than $y_{m,\mathrm{EIP}}^{\max}$ but less than $y_{m,2}^{\max}$ can still be processed by process 2, but the

throughput of the established EIP coalition will be capped at $y_{m,\mathrm{EIP}}^{\max}$ to ensure the highest *EP* achieved.

Note that the feasible operating range of individual processes differs from one another, depending on the nature of each process *p* (e.g., equipment capacity, costs, material, and energy conversions). Within the FE region ($y_{m,\mathrm{EIP}}^{\min} \leq y_m \leq y_{m,\mathrm{EIP}}^{\max}$), the EIP coalition can still be operated when y_m falls outside the range of one or multiple processes *p*. In such a case, when y_m surpasses $y_{m,p}^{\max}$ for a specific process *p*, the surplus material will not be operated for that particular process *p* due to the restriction in the design capacity. Meanwhile, when y_m drops below $y_{m,p}^{\min}$, all processes *p* are still operated at $y_{m,}$ although some of them may go under the range with negative EP_p. Such losses are compensated by the *EP* generated from other processes *p* to ensure the entire coalition's economic feasibility.

To assure the interest of each participating party (i.e., EP_p), it is recommended that the developed coalition is operated within the overlapping range between all processes *p*. Such a region is shaded in grey within the FE region and labelled as the GF range. In this region, the bottlenecking processes within a developed coalition can be determined. For instance, process 1 is the upper bottleneck, while process 2 is the lower bottleneck of the alliance formed in this illustrative example. The GF region can be expanded to accommodate a broader range of y_m by increasing $y_{m,1}^{\max}$, lowering $y_{m,2}^{\min}$, or combination of both. Such changes could be implemented by changing the design or debottlenecking individual process *p*, as discussed by Foong et al. (2019). Apart from that, FORA allows for the assessment of operational performance in process *p* and developed EIP coalition in terms of *UI* and *FI*. For a given y_m (solid line), the operational performance (i.e., UI_1, UI_2, UI_{EIP}, FI_1^{U}, FI_2^{U}, $FI_{\mathrm{EIP}}^{\mathrm{U}}$, FI_1^{L}, FI_2^{L}, and $FI_{\mathrm{EIP}}^{\mathrm{L}}$) can be determined. Note that high UI_1, UI_2, and UI_{EIP} values indicate that most processing capacity in each process

292 p and EIP coalition developed are utilised. On the other hand, high FI_1^{U}, FI_2^{U}, $FI_{\mathrm{EIP}}^{\mathrm{U}}$, FI_1^{L}, FI_2^{L},
293 and $FI_{\mathrm{EIP}}^{\mathrm{L}}$ values represent great flexibility in each process p and EIP coalition developed to
294 handle any potential changes in $y_{m,}$ and vice versa.

295 Note that for a given y_m, the magnitude of EP_1, EP_2, and EP_{EIP} may vary significantly.
296 EP_{EIP}, which is the summation of all EP_p, usually has the highest magnitude (refer to Eq. 8).
297 Typically, both EP_p and EP_{EIP} increase with y_m as more products are produced and sold to
298 generate higher profits. However, the rate at which EP_p and EP_{EIP} increase varies from one
299 another. For instance, EP_1, EP_2, and EP_{EIP} may increase by one, two, and ten units, respectively,
300 for every incremental unit in y_m. To overcome this issue, *EPI* is introduced and plotted against
301 $y_{m,}$ as shown in **Figure 1 (b)**. This allows the EP_p and EP_{EIP} to be estimated based on a given
302 y_m value (refer to Eqs. 20 and 21). The following section of this paper presents an oil palm-
303 based case study to illustrate the proposed approach.

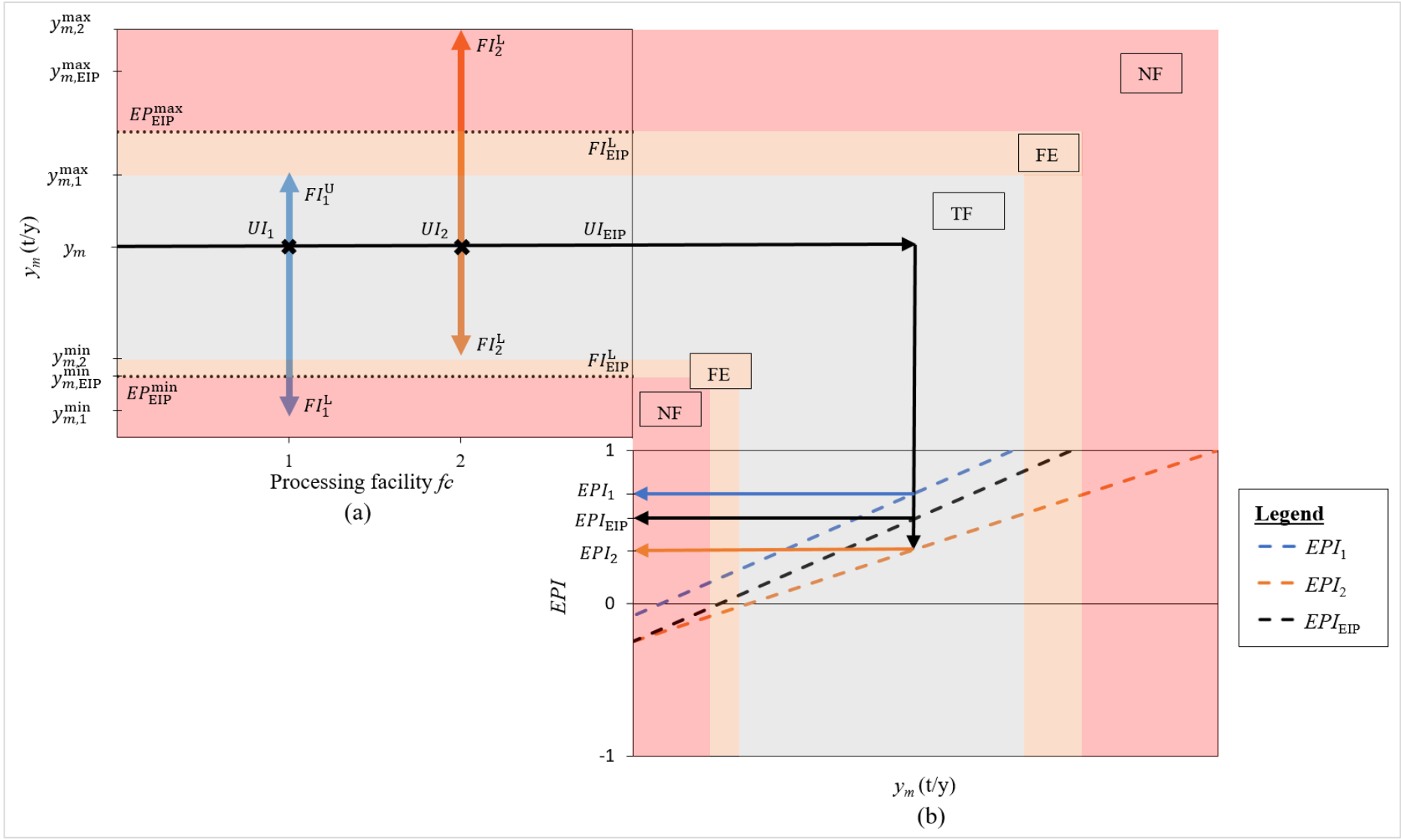

Figure 1. FORA illustration of an EIP coalition between two processes for (a) y_m, and (b) *EPI*

4. Case Study

In this case study, it is assumed that a mill owner has an existing POM as presented in Foong et al. (2018). Biomass is converted into bioenergy through combustion in a combined heat and power (CHP) system to fulfil the mill's demands of electricity and steam (Foong et al., 2019). It is further assumed that the mill owner is interested in investing in other processes around the POM to improve the overall economic performance while reducing the environmental impact. Such expansion includes biomass upgrading into value-added green products in a palm-based biorefinery (PBB) system (Deraman et al., 2002; GGS, 2018), and biogas generation from palm oil mill effluent (POME) while treating the waste effluent before discharge in an integrated biogas and wastewater (IBWT) system (Chin et al., 2013; Ohimain and Izah, 2017). Both processes can be integrated with the existing POM and CHP system to form an OPEIP coalition. Such interactions not only generate additional value but also satisfy the demands for energy while promotes the sustainability of the oil palm industry. Four different scenarios are proposed to consider every possible OPEIP configurations with the first scenario representing the baseline design, as shown in **Table 1**. The possible interactions within and between each process in the OPEIP coalition considered are provided in **Figure A.1** under the Supplementary Material.

Table 1. The specific coalition formed between processes in each scenario

Scenario	1	2	3	4
B_{POM}	1	1	1	1
B_{CHP}	1	1	1	1
B_{IBWT}	0	1	0	1
B_{PBB}	0	0	1	1

As shown, fresh fruit bunch (FFB) is used as raw materials in POM to produce products and by-products such as crude palm oil (CPO), palm kernel shell (PKS), POME, etc. These

328 materials can then be sold and utilised as feedstock in other processes. For instance, PKS and
329 palm pressed fibre (PPF) are sent to the CHP system for steam (i.e., low-pressure steam (LPS)
330 and medium-pressure steam (MPS)) and power generation. Steam generated from the CHP
331 system can be transferred back to the POM and PBB system to fulfil their demands for LPS
332 and MPS. Meanwhile, POME is treated in the IBWT system to reduce the wastewater
333 impurities while generating electricity from biogas captured. It is assumed that all the power
334 generated from CHP and IBWT systems are fed into the national grid at a premium rate under
335 the feed-in-tariff (FiT) scheme. In return, the electrical demand to operate each process is
336 obtained from the grid at a fixed price given by the power company. Alternatively, by-products
337 such as POME, PKS, and pressed empty fruit bunch (PEFB) can be processed in the PBB
338 system to generate other value-added green products.

339 The list of technologies considered for each process and their specifications are
340 provided in **Table A.1**. Additional information on material conversions in each process can be
341 obtained in the process matrix tables (**Tables A.2** – **A.5**). The costs of materials to sell or
342 purchase from external sources and other processes are summarised in **Table A.6**. The table
343 also provides the specific emissions rate for the production or disposal of material. In this work,
344 electricity purchased and sold to the national grid are assumed to be the same rate of 0.0796
345 US$/kWh (SEDA Malaysia, 2017). Note that the transportation costs to transfer raw materials
346 and final products to and from the site are not included in the price given as the supply chain
347 is not considered in this study. Materials exchanged between processes are free from
348 transportation costs based on the assumption that every plant is built on the same site. Besides,
349 the grid connection is assumed to be readily available on the site without any additional costs
350 required.

351 The OPEIP coalition is developed based on an average of 261,000 tonnes FFB
352 processed by the POM every year (y_{FFB} = -261,000). Each process is expected to operate for

15 years. A depreciation rate of 5 to 20% every year in capital invested is anticipated, due in particular to wear and tear of machinery purchased. In this study, a discount rate of 5% per annum is assumed. However, note that the basis used can be revised to accommodate for any adjustments in the future. A total of 12, 3, 5, and 5 operators are required to manage the plant operations for POM, CHP, IBWT, and PBB systems, respectively, at an average price of 15,250 US$/y per person. An MILP model was developed based on Eqs. 2 - 18 to establish an optimal OPEIP coalition network with an objective function given in Eq. 1.

5. Results and Discussion

Based on the proposed approach, the EP_{EIP} and GHG_{EIP} of each possible coalition in the OPEIP are determined. Each scenario is computed based on the specific coalition formed between various processes, as shown in **Table 1**. The model consists of 443 continuous variables with 34 integer variables and 577 constraints, solved within a second to achieve a global solution. The optimised OPEIP coalition networks are presented in **Figure 2**, with the results summarised in **Table 2**.

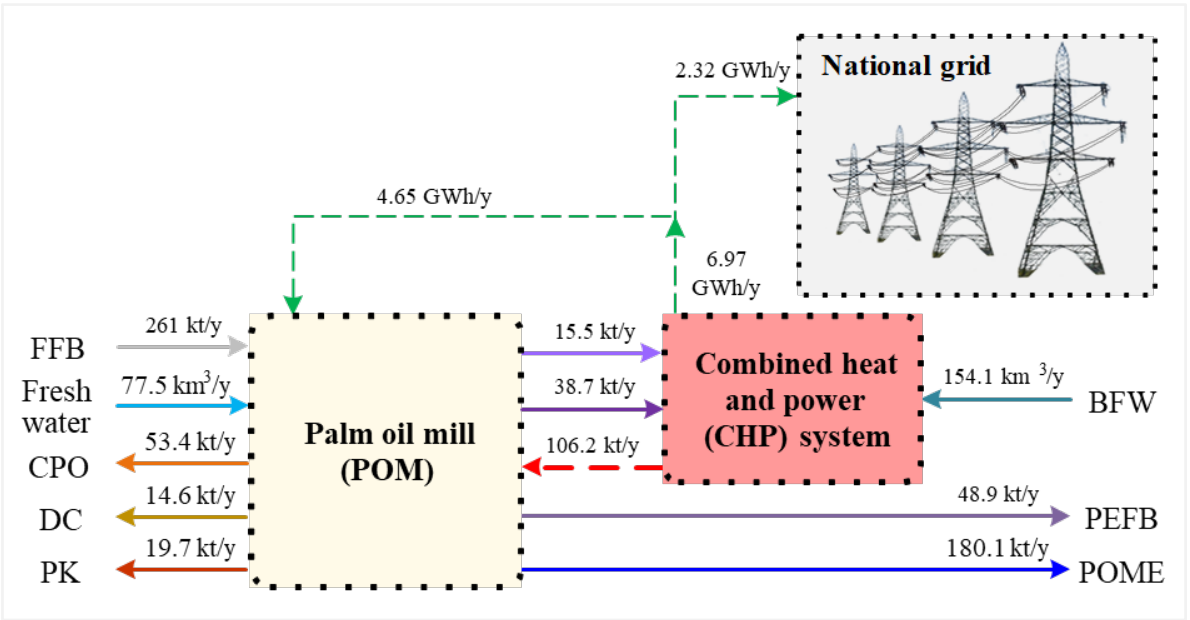

(a)

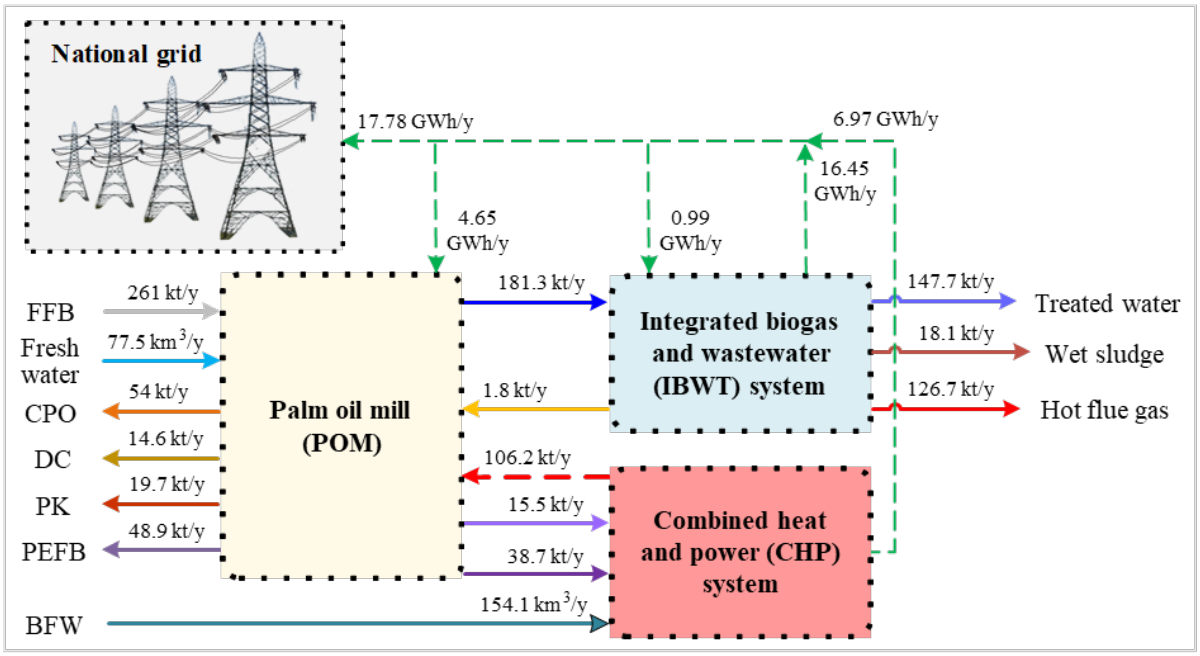
National grid
17.78 GWh/y
6.97 GWh/y
16.45 GWh/y
4.65 GWh/y
0.99 GWh/y
FFB
261 kt/y
Fresh water
77.5 km3/y
CPO
54 kt/y
DC
14.6 kt/y
PK
19.7 kt/y
PEFB
48.9 kt/y
BFW
Palm oil mill (POM)
181.3 kt/y
1.8 kt/y
106.2 kt/y
15.5 kt/y
38.7 kt/y
154.1 km3/y
Integrated biogas and wastewater (IBWT) system
Combined heat and power (CHP) system
147.7 kt/y
Treated water
18.1 kt/y
Wet sludge
126.7 kt/y
Hot flue gas

(b)

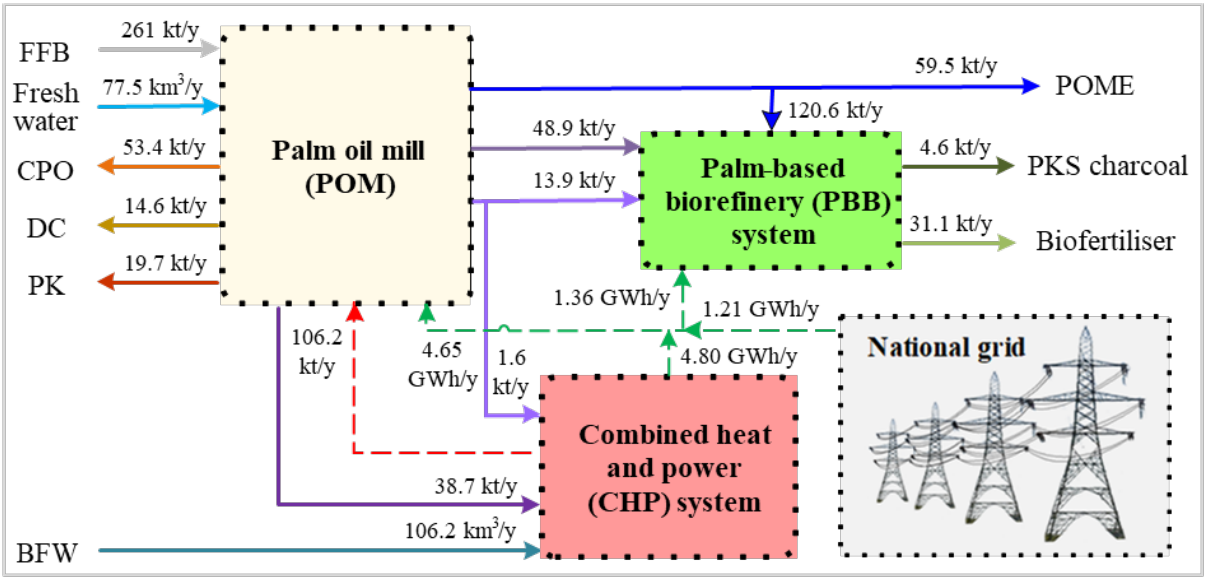
FFB
261 kt/y
Fresh water
77.5 km3/y
CPO
53.4 kt/y
DC
14.6 kt/y
PK
19.7 kt/y
BFW
Palm oil mill (POM)
59.5 kt/y
POME
120.6 kt/y
48.9 kt/y
13.9 kt/y
Palm-based biorefinery (PBB) system
4.6 kt/y
PKS charcoal
31.1 kt/y
Biofertiliser
1.36 GWh/y
1.21 GWh/y
4.80 GWh/y
106.2 kt/y
4.65 GWh/y
1.6 kt/y
38.7 kt/y
106.2 km3/y
Combined heat and power (CHP) system
National grid

(c)

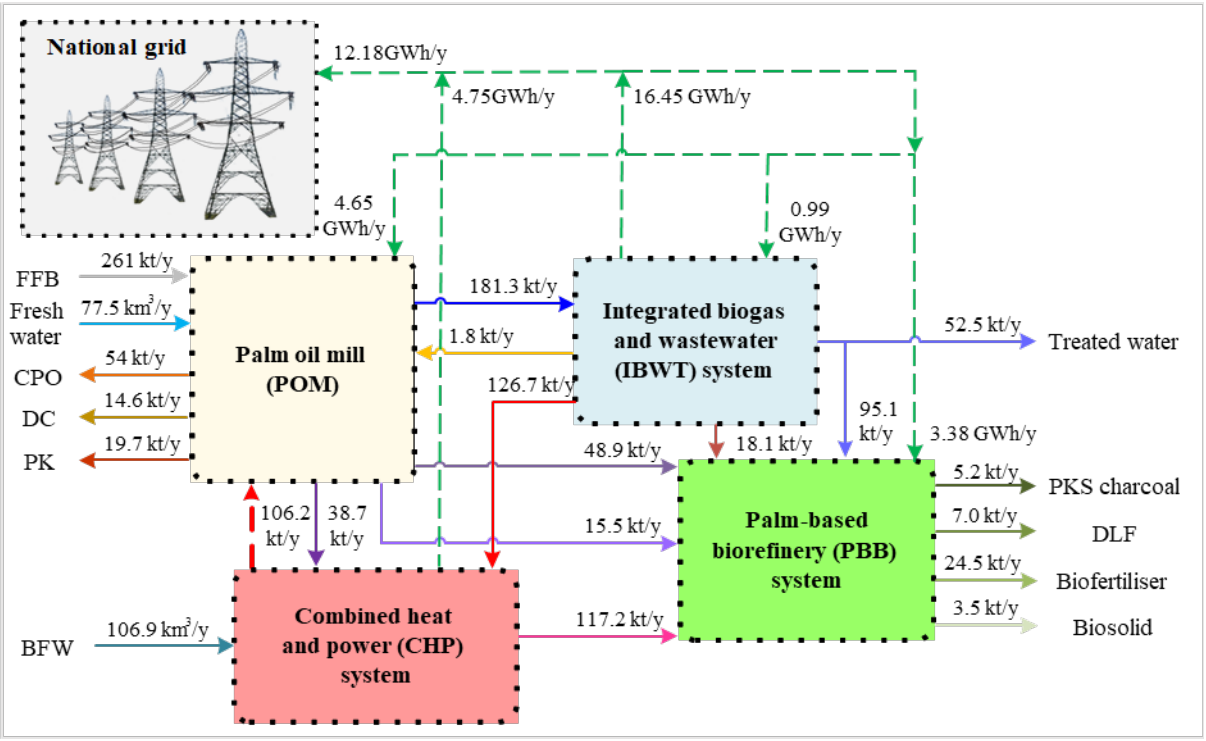

(d)

Figure 2. OPEIP network developed for scenario (a) 1, (b) 2, (c) 3, and (d) 4

Table 2. Optimised results for OPEIP coalition developed

Scenario	1	2	3	4
$CAPEX_{EIP}$ (million US$)	11.56	15.17	16.03	18.96
$OPEX_{EIP}$ (million US$/y)	1.21	1.49	2.71	3.16
GP_{EIP} (million US$/y)	5.68	6.72	7.19	8.71
EP_{EIP} (million US$/y)	4.57	5.26	5.65	6.88
EP_{POM} (million US$/y)	4.40	4.75	4.40	4.75
EP_{CHP} (million US$/y)	0.050	0.050	0.035	0.030
EP_{IBWT} (million US$/y)	-	0.51	-	0.51
EP_{PBB} (million US$/y)	-	-	1.30	1.65
GHG_{EIP} (kt CO_{2e}/y)	199.88	157.22	75.67	63.29
GHG_{POM} (kt CO_{2e}/y)	149.75	150.13	149.75	150.13
GHG_{CHP} (kt CO_{2e}/y)	50.13	50.13	46.82	46.43
GHG_{IBWT} (kt CO_{2e}/y)	-	-43.04	-	-43.04
GHG_{PBB} (kt CO_{2e}/y)	-	-	-120.90	-90.23
Benefit-cost ratio, *BCR*	1.00	2.99	3.51	4.24
Carbon saving, *CS* (kt CO_{2e}/million US$/y)	1.00	11.82	27.82	18.46

In Scenario 1, an alliance is formed between POM and CHP system with the optimised results of EP_{EIP} is determined as 4.57 million US$/y. It is noted that all the PKS and PPF by-products (15.5 and 38.7 kt/y) are utilised in the CHP system to generate 6.97 GWh/y of electricity. This gives a net output of 2.32 GWh/y (=6.97 – 4.65 GWh/y) electrical power to the national grid while fulfilling the LPS demand of 106.2 kt/y needed to operate the POM. A total of 199.88 kt CO_{2e}/y of GHG_{EIP} is reported, where 149.75 and 50.13 kt CO_{2e}/y are emitted by POM and CHP system, respectively. Carbon is emitted in the POM due to the disposal of by-products such as POME, PEFB, and decanter cake (DC). Meanwhile, the CHP system's carbon emissions are mainly due to the combustions of PKS and PPF in the boiler for steam generation.

For Scenario 2, the IBWT system is included in the OPEIP coalition formed, generating an EP_{EIP} of 5.26 million US$/y. The operations of the POM and CHP system remain unchanged in the presence of IBWT system, however, POME is treated in the IBWT system to produce treated water and wet sludge while generating an additional 15.45 GWh/y (=16.45 – 0.99 GWh/y) electricity. After fulfilling the electricity needed in the milling process, a n excess of 17.78 GWh/y electricity is exported to the national grid. Besides, 1.8 kt/y of oil is recovered in the IBWT system, which increases the CPO output in POM by 0.6 kt/y (=54 – 53.4 kt/y). In the presence of the IBWT system in Scenario 2, GHG_{EIP} is reduced to 157.22 kt CO_{2e}/y as 43.04 kt CO_{2e}/y is trapped as biogas and combusted for power generation. It is worth mentioning that the difference in GHG_{EIP} is mainly due to the removal of methane gas with a global warming potential 25 times higher than carbon dioxide (Gardner et al., 1993), released directly to the atmosphere.

Meanwhile, a coalition is formed among POM, CHP, and PBB systems in Scenario 3 reported an EP_{EIP} of 5.65 million US$/y. In this coalition, PEFB and POME are converted into 31.1 kt/y of biofertilisers through the PBB system. Besides, only a small portion of PKS (1.6

kt/y) is utilised in the CHP system to ensure sufficient LPS to sustain the mill's operation. Most of the PKS (13.9 kt/y) is sold to the PBB system for PKS charcoal productions. As a result, the CHP system's power reduces significantly (4.8 GWh/y as compared to 6.97 GWh/y earlier), and therefore, lesser boiler feedwater at 106.2 km^3/y is required. Meanwhile, 1.36 GWh/y of electricity is necessary to operate the PBB system. In this respect, the net output of electricity from the coalition formed falls to -1.21 GWh/y (=4.8 – 4.65 – 1.36 GWh/y), where power is imported from the national grid to sustain the operations of the coalition formed. In this scenario, only 75.67 kt CO_{2e}/y of GHG_{EIP} is reported as the PBB system reduces 120.9 kt CO2e/y. Lesser carbon is emitted in the CHP system due to the smaller amount of PKS being combusted for power generation. Besides, carbons in by-products such as POME, PEFB, and PKS are trapped during the production of biofertiliser and PKS charcoal.

Lastly, in Scenario 4, an alliance among all four processes is formed and generates an EP_{EIP} of 6.88 million US$/y. The result shows that all the PKS from POM (15.5 kt/y) is converted into PKS charcoal in the PBB system. Hot flue gas from the IBWT system is utilised in the CHP system to generate sufficient LPS to operate the milling process. Hot air is then used in the PBB system for dry long fibre (DLF) productions. Due to insufficient heating duty from the CHP system, only 7.0 kt/y of DLF can be produced while the remaining PEFB will be composted to form biofertilisers. The POM, IBWT, and PBB systems require 4.65, 0.99, and 3.38 GWh/y electricity, respectively. At the same time, 4.75 and 16.45 GWh/y are generated from CHP and IBWT system, giving a positive net output of 12.18 GWh/y electricity exported to the national grid. GHG_{EIP} is further reduced to 63.29 kt CO_{2e}/y, where 43.04 and 90.23 kt CO_{2e}/y is reduced by the IBWT and PBB systems, respectively.

A better illustration of the changes in economic and environmental aspects for each scenario is provided in **Figure 3**. The performance improvement can be indicated by the

benefit-cost ratio, *BCR,* and carbon saving, *CS* via Eqs. 27 and 28 to evaluate the effectiveness of additional investment made.

$$BCR = \frac{GP_{\text{EIP}} - GP_{\text{EIP 1}}}{\text{CRF}(\text{CAPEX}_{\text{EIP}} - \text{CAPEX}_{\text{EIP 1}})} \tag{27}$$

$$CS = \frac{GHG_{\text{EIP}} - GHG_{\text{EIP 1}}}{\text{CAPEX}_{\text{EIP}} - \text{CAPEX}_{\text{EIP 1}}} \tag{28}$$

By setting Scenario 1 as the baseline for the OPEIP coalition formed, Scenario 4 shows the most promising investment in terms of economic aspect as the greatest *BCR* of 4.24 is achieved. It is relatively more cost-effective to invest in both IBWT and PBB systems to make the most significant economic benefit within the OPEIP coalition. The environmental aspect, on the other hand, shows that Scenario 3 is a better option with the highest *CS* of 27.82 kt CO_{2e}/million US$/y. This indicates that the PBB system should be prioritised in the OPEIP coalition to reduce the GHG emissions under a restricted capital investment.

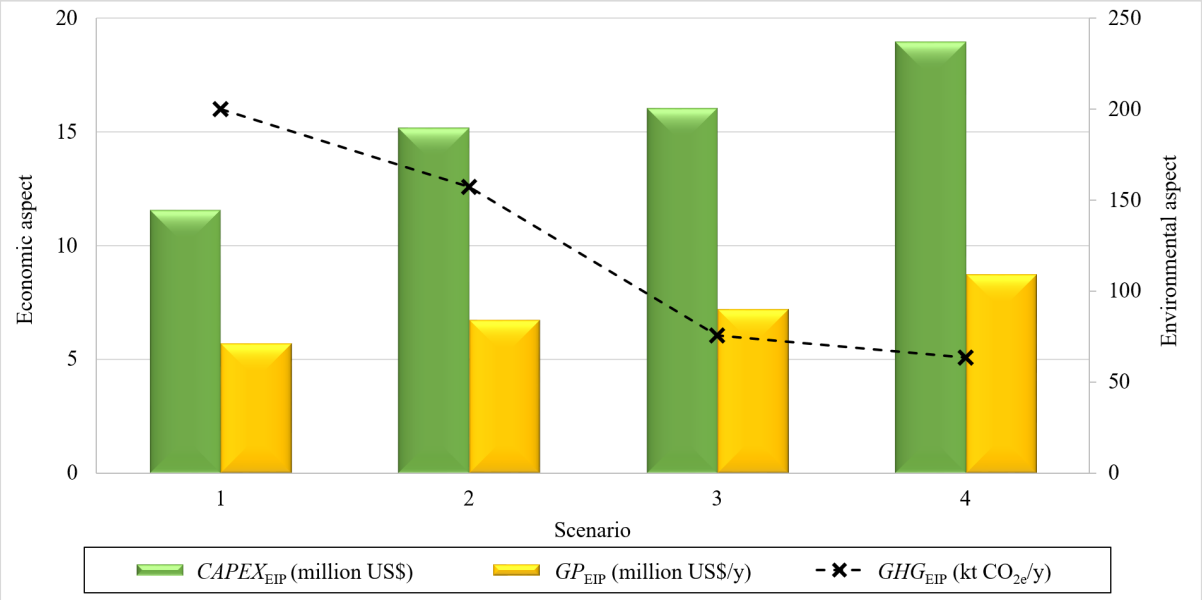

Figure 3. Changes in economic and environmental aspects with different scenarios

Next, FORA is performed on the OPEIP coalition formed in Scenario 4, subject to the constraints given in Eqs. 19 and 20. **Table A.7** summarises the $EP^{\max}$, $y_{\text{FFB}}^{\max}$, and $y_{\text{FFB}}^{\min}$ for

different processes and coalition formed. Following that, the changes in *EP* and *EPI* with y_{FFB} are determined from y_{FFB}^{max} (485.1 kt/y) to y_{FFB}^{min} (63.2 kt/y) at every 20 kt/y intervals, as shown in **Table A.8**. Note that the y_{FFB}^{max} and y_{FFB}^{min} are highlighted in green and red colours, respectively. Graphical representations for FORA is presented in **Figure 4.** Based on **Figure 4 (a)**, we can see that the FE region of the entire OPEIP coalition falls within 90.6 and 388.9 kt/y, where positive EP_{EIP} is generated. Meanwhile, when y_{FFB}.drops outside of this range, the alliance formed becomes economically unfeasible as negative EP_{EIP} is achieved and labelled as the NF region. However, to ensure the economic feasibility of each process within the coalition formed, the range of y_{FFB} is narrowed down to 250 and 371.6 kt/y (GF region). *EPI* is formulated based on the *EP* (refer to Eqs. 21 and 22) and plotted against y_{FFB}. **Figure 4 (b)** reveals that a reasonably accurate *EPI* could be estimated, EPI^{Est} using Eqs. 29 – 33 for any given y_{FFB} value with a coefficient of determination, R^2 more than 0.99.

$$EPI_{POM}^{Est} = 0.003\ (-y_{FFB}) - 0.1759 \qquad (R^2 = 0.9987) \qquad (29)$$

$$EPI_{CHP}^{Est} = 0.0049\ (-y_{FFB}) - 1.224 \qquad (R^2 = 0.9994) \qquad (30)$$

$$EPI_{IBWT}^{Est} = 0.0044\ (-y_{FFB}) - 0.6488 \qquad (R^2 = 0.9996) \qquad (31)$$

$$EPI_{PBB}^{Est} = 0.0027\ (-y_{FFB}) - 0.216 \qquad (R^2 = 0.9922) \qquad (32)$$

$$EPI_{EIP}^{Est} = 0.0033\ (-y_{FFB}) - 0.2981 \qquad (R^2 = 0.9994) \qquad (33)$$

Table A.9 summarises the *UI*, *FI*, *EP*, and *EPI* of each process, and the OPEIP coalition formed when 261 kt/y of FFB is processed (solid black line). Note that a reasonably accurate *EPI* can be estimated via the formulae provided with a maximal difference of only 0.014 as compared to the actual value of 0.485 for the IBWT system. This indicates that such analysis allows the *EP* to be estimated without any significant error, and therefore, reduces the time and effort required to recompute the process as y_{FFB} changes.

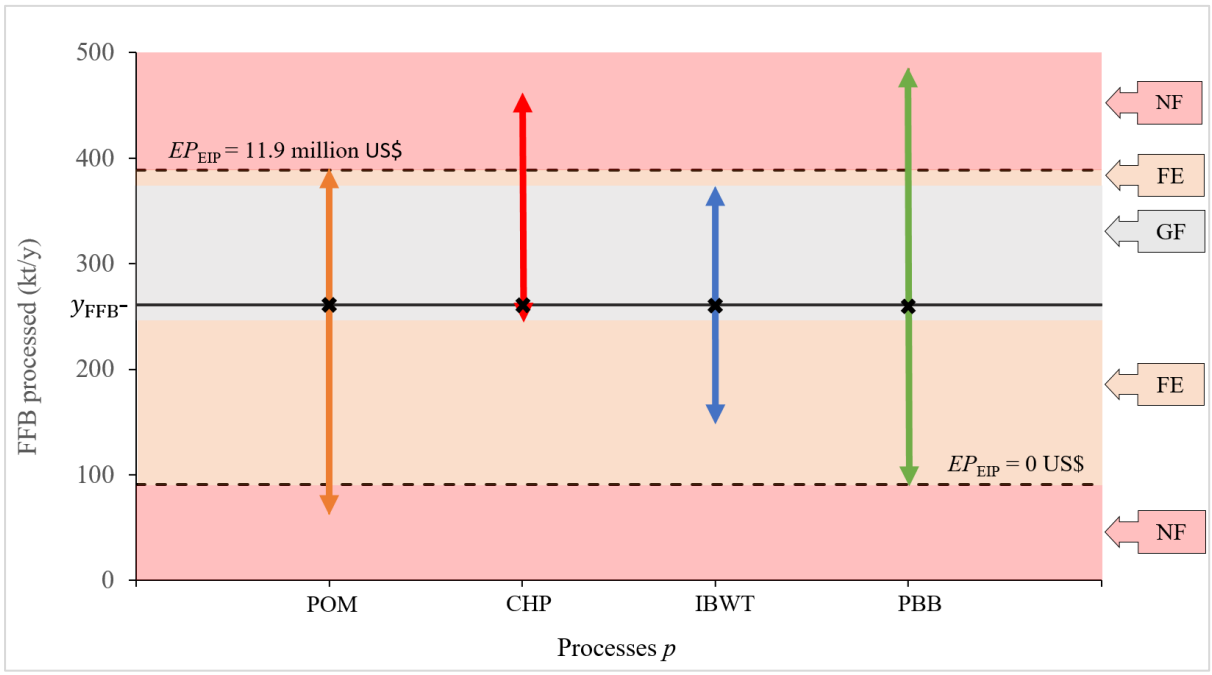

(a)

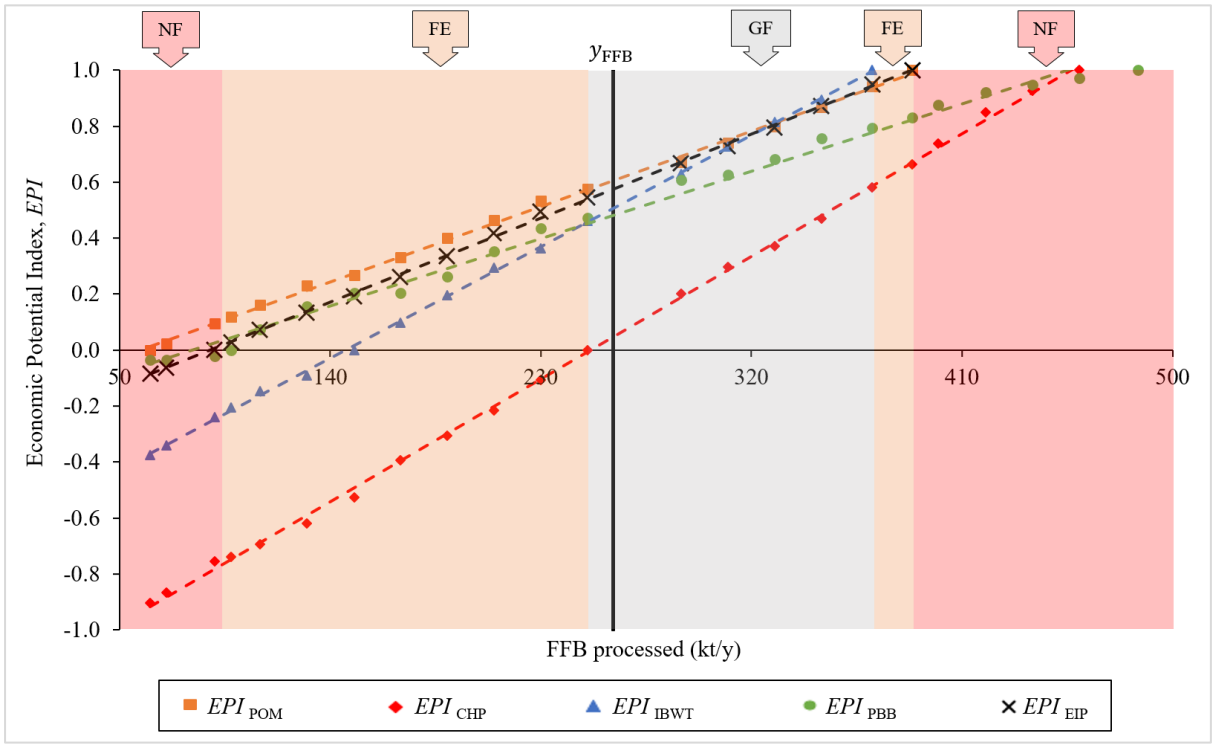

(b)

Figure 4. Graphical representation of FORA for (a) y_{FFB}, and (b) *EPI* of the EIP coalition formed

6. Conclusion

A general MILP model with FORA is established to develop an EIP coalition. In this paper, an oil palm-based case study is presented and solved to illustrate the proposed approach. A graphical representation is used to show the changes in operational performance, such as utilisation, flexibility, and economic performance for individual processes, as well as the alliance formed with respect to the changes in material processed. The results demonstrated that the EP_{EIP} can be improved from 4.57 to 6.88 million US$/y with an OPIS coalition consisting of all four processes. At the same time, GHG_{EIP} is also reduced significantly from 199.88 to 63.29 kt CO_{2e}/y.It is shown that the PBB process is more effective in reducing the GHG emissions (CS = 27.82kt CO_{2e}/million US$/y) than the IBWT system (CS = 11.82kt CO_{2e}/million US$/y) in the oil palm industry. On the other hand, multiple-processes FORA allows the measurement of utilisation and flexibility for individual processes and EIP coalition developed, as well as estimating the changes in EP_p and EP_{EIP} accurately with respect to the changes in FFB feedstock processed. Future work will focus on extending the proposed approach to consider the supply chain and effects of uncertainties in real-world applications such as the changes in raw materials availability, product demand, and material prices.

Author contributions

Steve Z.Y. Foong: Conceptualisation, Data curation, Formal analysis, Investigation, Software, Methodology, Visualisation, Writing - Original draft. **Denny K.S. Ng:** Funding acquisition, Project administration, Resources, Supervision, Validation, Writing - review & editing.

Supplementary material

E-supplementary data of this work can be found in the online version of this paper.

Acknowledgements

This work was financially supported by the Ministry of Higher Education, Malaysia [LRGS/2013/UKM-UNMC/PT/05].

Nomenclature

Abbreviation	Description
BFW	Boiler Feed Water
CHP	Combined Heat and Power
CPO	Crude Palm Oil
DC	Decanter Cake
DLF	Dry Long Fibre
EIP	Eco-Industrial Park
FE	Feasible
FFB	Fresh Fruit Bunch
FiT	Feed-in-Tariff
FORA	Feasible Operating Range Analysis
GF	Global Feasible
GHG	Greenhouse Gas
IBWT	Integrated Biogas and Wastewater Treatment
IS	Industrial Symbiosis
LP	Linear Programming
LPS	Low-Pressure Steam
MILP	Mixed-Integer Linear Programming
MINLP	Mixed-Integer Non-Linear Programming
MPS	Medium-Pressure Steam
NF	Not Feasible
OPEIP	Oil palm-based Eco-Industrial Park
PBB	Palm-based Biorefinery
PEFB	Pressed Empty Fruit Bunch
PI	Process Integration
PKS	Palm Kernel Shell
POM	Palm Oil Mill
POME	Palm Oil Mill Effluent
POPC	Palm Oil Processing Complex
PPF	Palm Pressed Fibre
SEDA	Sustainable Energy Development Authority

Sets	Description
e	Index for electricity
m	Index for material
p	Index for process
te	Index for technology

Variables	Description
BCR	Benefit-cost ratio
CS	Carbon saving
$E_{e,\mathrm{EIP}}^{\mathrm{Demand}}$	Total electricity demand for EIP coalition
$E_{e,p}^{\mathrm{Demand}}$	Total electricity demand for process p
$E_{e,\mathrm{PBB}}^{\mathrm{Demand}}$	Total electricity demand for PBB system
EP_1	Economic performance for process 1
EP_2	Economic performance for process 2
EP_{CHP}	Economic performance for CHP system
EP_{EIP}	Economic performance for EIP coalition
$EP^{\max}$	Maximum economic performance for process 1
$EP_{\mathrm{EIP}}^{\max}$	Maximum economic performance for EIP coalition
$EP_p^{\max}$、	Maximum economic performance for process p
EP_p	Economic performance for process p
EPI^{Est}	Estimated economic performance
EP_{PBB}	Economic performance for PBB system
EPI	Economic performance index
EPI_{CHP}	Economic performance index for CHP system
$EPI_{\mathrm{CHP}}^{\mathrm{Est}}$	Estimated economic performance for CHP system
$EPI_{\mathrm{IBWT}}^{\mathrm{Est}}$	Estimated economic performance for IBWT system
$EPI_{\mathrm{EIP}}^{\mathrm{Est}}$	Estimated economic performance EIP coalition
$EPI_{\mathrm{PBB}}^{\mathrm{Est}}$	Estimated economic performance for PBB system
$EPI_{\mathrm{POM}}^{\mathrm{Est}}$	Estimated economic performance for POM
EP_{IBWT}	Economic performance for IBWT system
EPI_{IBWT}	Economic performance index for IBWT system
EPI_{PBB}	Economic performance index for PBB system
EPI_{POM}	Economic performance index for POM
EP_{POM}	Economic performance index for POM
FI	Flexibility index
FI^{L}	Lower flexibility index
FI_1^{L}	Lower flexibility index for process 1

571	FI_2^{L}	Lower flexibility index for process 2
572	$FI_{\mathrm{EIP}}^{\mathrm{L}}$	Lower flexibility index for EIP coalition
573	FI_p^{L}	Lower flexibility index for process *p*
574	FI^{U}	Upper flexibility index
575	FI_1^{U}	Upper flexibility index for process 1
576	FI_2^{U}	Upper flexibility index for process 2
577	$FI_{\mathrm{EIP}}^{\mathrm{U}}$	Upper flexibility index for EIP coalition
578	FI_p^{U}	Upper flexibility index for process *p*
579	GHG_{CHP}	Greenhouse gas emissions from CHP system
580	GHG_{EIP}	Greenhouse gas emissions from EIP coalition
581	GHG_{IBWT}	Greenhouse gas emissions from IBWT system
582	GHG_p	Greenhouse gas emissions from process *p*
583	GHG_{PBB}	Greenhouse gas emissions from PBB system
584	GHG_{POM}	Greenhouse gas emissions from POM
585	GP_{EIP}	Gross profit for EIP coalition
586	GP_p	Gross profit for process *p*
587	$OPEX_{\mathrm{EIP}}$	Total operating costs for EIP coalition
588	$OPEX_p$	Total operating costs for process *p*
589	R^2	Coefficient of determination
590	UI	Utilisation index
591	UI_1	Utilisation index for process 1
592	UI_2	Utilisation index for process 2
593	UI_{EIP}	Utilisation index for EIP coalition
594	UI_p	Utilisation index for process *p*
595	$\boldsymbol{U}_{te,p}$	Vector for number of equipment units for technology *te* operated in process *p*
596	$\boldsymbol{x}_{te,p}$	Vector for the processing capacity of technology *te* in process *p*
597	$y_{e,\mathrm{EIP}}$	Electricity input or output for EIP coalition
598	$y_{e,p}$	Electricity input or output for process *p*
599	y_{FFB}	Input or output flowrate of FFB
600	y_m	Input or output flowrate of material *m*
601	$y_{\mathrm{FFB}}^{\max}$	Maximum input or output flowrate of FFB
602	$y_{m,1}^{\max}$	Maximum input or output flowrate of material *m* for process 1
603	$y_{m,2}^{\max}$	Maximum input or output flowrate of material *m* for process 2
604	$y_{m,\mathrm{EIP}}^{\max}$	Maximum input or output flowrate of material *m* for EIP coalition
605	$\boldsymbol{y}_{m,\mathrm{EIP}}^{\max}$	Vector for maximum input or output flowrate of material *m* for EIP coalition
606	$y_{m,p}^{\max}$	Maximum input or output flowrate of material *m* for process *p*

$\boldsymbol{y}_{m,p}^{\max}$	Vector for maximum input or output flowrate of material *m* for process *p*
$y_{\mathrm{FFB}}^{\min}$	Minimum input or output flowrate of FFB
$y_{m,1}^{\min}$	Minimum input or output flowrate of material *m* for process 1
$y_{m,2}^{\min}$	Minimum input or output flowrate of material *m* for process 2
$y_{m,\mathrm{EIP}}^{\min}$	Minimum input or output flowrate of material *m* for EIP coalition
$\boldsymbol{y}_{m,\mathrm{EIP}}^{\min}$	Vector for minimum input or output flowrate of material *m* for EIP coalition
$y_{m,p}^{\min}$	Minimum input or output flowrate of material *m* for process *p*
$\boldsymbol{y}_{m,p}^{\min}$	Vector for minimum input or output flowrate of material *m* for process *p*
$y_{m,\mathrm{EIP}}$	Input or output flowrate of material *m* for EIP coalition
$\boldsymbol{y}_{m,\mathrm{EIP}}$	Vector for input or output flowrate of material *m* for EIP coalition
$y_{m,p}$	Input or output flowrate of material *m* for process *p*
$\boldsymbol{y}_{m,p}$	Vector for input or output flowrate of material *m* for process *p*

Parameters	Description
$\mathbf{A}_{m,te,p}$	Input and output matrix between material *m* and technology *te* for process *p*
$\mathrm{B_{CHP}}$	Binary parameter for CHP system
$\mathrm{B_{IBWT}}$	Binary parameter for IBWT system
$\mathbf{B}_p$	Set for binary parameters for process *p*
$\mathrm{B_{PBB}}$	Binary parameter for PBB system
$\mathrm{B_{POM}}$	Binary parameter for POM
$\mathrm{CAPEX_{EIP}}$	Total capital costs for EIP coalition
CAPEX_p	Total capital costs for process *p*
$\mathbf{CAP}_{te,p}$	Set for nominal capacity of technology *te* for process *p*
$\mathbf{CC}_{te,p}$	Diagonal matrix for capital costs of technology *te* for process *p*
C_e^{Imp}	Cost of electricity *e* imported
$\mathrm{C_{lab}}$	Cost of labour
$\mathbf{C}_m$	Set for costs of material *m*
CRF	Capital recovery factor
$\mathbf{E}_{te,p}$	Diagonal matrix for electricity consumption specified per unit technology *te* for process *p*
LC_p	Total labour costs for process *p*
$\mathrm{n_{wk,}}_p$	Number of workers for process *p*
$\mathbf{OC}_{te,p}$	Diagonal matrix for operating and maintenance costs of technology *te* for process *p*
r	Discount rate
$\mathbf{SER}_m$	Specific emissions rate for material *m*

643 t_{te}^{max} Maximum operational lifespan for technology *te*

644 $\mathbf{U}_{te,p}^{max}$ Set for maximum units of technology *te* installed for process *p*

645

646 References

647 Andiappan, V., Ng, D.K.S., Tan, R.R., 2017. Design Operability and Retrofit Analysis (DORA)
648 Framework for Energy Systems. Energy 134, 1038–1052.
649 https://doi.org/10.1016/j.energy.2017.06.054

650 Andiappan, V., Tan, R.R., Ng, D.K.S., 2016. An Optimisation-based Negotiation Framework
651 for Energy Systems in an Eco-Industrial Park. J. Clean. Prod. 129, 496–507.
652 https://doi.org/10.1016/J.JCLEPRO.2016.04.023

653 Aviso, K.B., Tan, R.R., Culaba, A.B., Cruz, J.B., 2010. Bi-level Fuzzy Optimisation Approach
654 for Water Exchange in Eco-Industrial Parks. Process Saf. Environ. Prot. 88, 31–40.
655 https://doi.org/10.1016/J.PSEP.2009.11.003

656 Azman, I., 2014. The Impact of Palm Oil Mills' Capacity on Technical Efficiency of Palm Oil
657 Millers in Malaysia. Oil Palm Ind. Econ. J. 14, 35–41.

658 Bade, M.H., Bandyopadhyay, S., 2014. Minimization of Thermal Oil Flow Rate for Indirect
659 Integration of Multiple Plants. Ind. Eng. Chem. Res. 53, 13146–13156.
660 https://doi.org/10.1021/ie502059f

661 Bandyopadhyay, S., Varghese, J., Bansal, V., 2010. Targeting for Cogeneration Potential
662 Through Total Site Integration. Appl. Therm. Eng. 30, 6–14.
663 https://doi.org/10.1016/j.applthermaleng.2009.03.007

664 Chae, S.H., Kim, S.H., Yoon, S.G., Park, S., 2010. Optimization of a Waste Heat Utilization
665 Network in an Eco-Industrial Park. Appl. Energy 87, 1978–1988.
666 https://doi.org/10.1016/j.apenergy.2009.12.003

667 Chertow, M.R., 2007. "Uncovering" Industrial Symbiosis. J. Ind. Ecol. 11, 11–30.
668 https://doi.org/10.1162/jiec.2007.1110

669 Chertow, M.R., 2000. Industrial Symbiosis: Literature and Taxonomy. Annu. Rev. Energy
670 Environ. 25, 313–337. https://doi.org/10.1146/annurev.energy.25.1.313

671 Chertow, M.R., Ashton, W.S., Espinosa, J.C., 2008. Industrial Symbiosis in Puerto Rico:
672 Environmentally Related Agglomeration Economies. Reg. Stud. 42, 1299–1312.
673 https://doi.org/10.1080/00343400701874123

674 Chew, I.M.L., Foo, D.C.Y., 2009. Automated Targeting for Inter-Plant Water Integration.
675 Chem. Eng. J. 153, 23–36. https://doi.org/10.1016/j.cej.2009.05.026

676 Chew, I.M.L., Tan, R., Ng, D.K.S., Foo, D.C.Y., Majozi, T., Gouws, J., 2008. Synthesis of
677 Direct and Indirect Interplant Water Network. Ind. Eng. Chem. Res. 47, 9485–9496.
678 https://doi.org/10.1021/ie800072r

679 Chin, M.J., Poh, P.E., Tey, B.T., Chan, E.S., Chin, K.L., 2013. Biogas from Palm Oil Mill
680 Effluent (POME): Opportunities and Challenges from Malaysia's perspective. Renew.
681 Sustain. Energy Rev. 26, 717–726. https://doi.org/10.1016/J.RSER.2013.06.008

682 Deng, C., Zhou, Y., Chen, C.L., Feng, X., 2015. Systematic Approach for Targeting Interplant

683 Hydrogen Networks. Energy 90, 68–88. https://doi.org/10.1016/j.energy.2015.05.054

684 Deng, C., Zhou, Y., Jiang, W., Feng, X., 2017. Optimal Design of Inter-Plant Hydrogen
685 Network with Purification Reuse/Recycle. Int. J. Hydrogen Energy 42, 19984–20002.
686 https://doi.org/10.1016/j.ijhydene.2017.06.199

687 Deraman, M., Omar, R., Zakaria, S., Mustapa, I.R., Talib, M., Alias, N., Jaafar, R., 2002.
688 Electrical and Mechanical Properties of Carbon Pellets from Acid (HNO3) Treated Self-
689 Adhesive Carbon Grain from Oil Palm Empty Fruit Bunch. J. Mater. Sci. 37, 3329–3335.
690 https://doi.org/10.1023/A:1016525106663

691 Ehrenfeld, J., Gertler, N., 1997. Industrial Ecology in Practice: The Evolution of
692 Interdependence at Kalundborg. J. Ind. Ecol. 1, 67–79.
693 https://doi.org/10.1162/jiec.1997.1.1.67

694 El-Halwagi, M.M., 2017. A Shortcut Approach to the Multi-Scale Atomic Targeting and
695 Design of C–H–O Symbiosis Networks. Process Integr. Optim. Sustain. 1, 3–13.
696 https://doi.org/10.1007/s41660-016-0001-y

697 Enríquez-Gutiérrez, V.M., Jobson, M., Ochoa-Estopier, L.M., Smith, R., 2015. Retrofit of
698 Heat-Integrated Crude Oil Distillation Columns. Chem. Eng. Res. Des. 99, 185–198.
699 https://doi.org/10.1016/J.CHERD.2015.02.008

700 Fadzil, A.F.A., Alwi, S.R.W., Manan, Z.A., Klemeš, J.J., 2017. Total Site Centralised Water
701 Integration for Efficient Industrial Site Water Minimisation. Chem. Eng. Trans. 61, 1141–
702 1146. https://doi.org/10.3303/CET1761188

703 Foong, S.Z.Y., Andiappan, V., Tan, R.R., Foo, D.C.Y., Ng, D.K.S., 2019. Hybrid Approach
704 for Optimisation and Analysis of Palm Oil Mill. Processes 7, 1–27.
705 https://doi.org/10.3390/pr7020100

706 Foong, S.Z.Y., Lam, Y.L., Andiappan, V., Foo, D.C.Y., Ng, D.K.S., 2018. A Systematic
707 Approach for the Synthesis and Optimization of Palm Oil Milling Processes. Ind. Eng.
708 Chem. Res. 57, 2945–2955. https://doi.org/10.1021/acs.iecr.7b04788

709 Gardner, N., Manley, B.J.W., Pearson, J.M., 1993. Gas Emissions from Landfills and Their
710 Contributions to Global Warming. Appl. Energy 44, 165–174.
711 https://doi.org/10.1016/0306-2619(93)90059-X

712 Global Green Synergy (GGS), 2018. Palm Dried Long Fiber [WWW Document]. URL
713 https://www.ggs.my/ggs-products/palm-dried-long-fiber (accessed 5.27.19).

714 Grossmann, I.E., Halemane, K.P., Swaney, R.E., 1983. Optimisation Strategies for Flexible
715 Chemical Processes. Comput. Chem. Eng. 7, 439–462. https://doi.org/10.1016/0098-
716 1354(83)80022-2

717 Grossmann, I.E., Morari, M., 1983. Operability, Resiliency, and Flexibility: Process Design
718 Objectives for a Changing World. Design Research Center, Carnegie-Mellon University.

719 Jiang, W., Zhang, Z., Deng, C., Tang, X., Feng, X., 2019. Industrial Park Water System
720 Optimization with Joint Use of Water Utility Sub-System. Resour. Conserv. Recycl. 147,
721 119–127. https://doi.org/10.1016/j.resconrec.2019.04.005

722 Kamat, S., Bandyopadhyay, S., 2019. Synthesis of Heat-Integrated Water Allocation Networks
723 Through Pinch Analysis. Process Integr. Optim. Sustain. 3, 515–531.
724 https://doi.org/10.1007/s41660-019-00096-5

725 Kasivisvanathan, H., Tan, R.R., Ng, D.K.S., Abdul Aziz, M.K., Foo, D.C.Y., 2014. Heuristic
726 Framework for the Debottlenecking of A Palm Oil-Based Integrated Biorefinery. Chem.

727 Eng. Res. Des. 92, 2071–2082. https://doi.org/10.1016/J.CHERD.2014.02.024

728 Kazmer, D., Hatch, D., Zhu, L., Roser, C., Kapoor, D., 2003. Definition and Application of a
729 Process Flexibility Index. J. Manuf. Sci. Eng. Trans. ASME 125, 164–171.
730 https://doi.org/10.1115/1.1536174

731 Kittrell, J.., Watson, C.., 1966. Don't Overdesign Process Equipment. Chem. Eng. Prog. 62,
732 79–83.

733 Lai, S.M., Hui, C.W., 2009. Feasibility and Flexibility for a Trigeneration System. Energy 34,
734 1693–1704. https://doi.org/10.1016/J.ENERGY.2009.04.024

735 Lee, S.H., Ng, R.T.L., Ng, D.K.S., Foo, D.C.Y., Chew, I.M.L., 2014. Synthesis of Resource
736 Conservation Networks in an Integrated Pulp and Paper Biorefinery. Ind. Eng. Chem. Res.
737 53, 10417–10428. https://doi.org/10.1021/ie404002r

738 Leong, Y.T., Tan, R.R., Aviso, K.B., Chew, I.M.L., 2016. Fuzzy Analytic Hierarchy Process
739 and Targeting for Inter-Plant Chilled and Cooling Water Network Synthesis. J. Clean.
740 Prod. 110, 40–53. https://doi.org/10.1016/j.jclepro.2015.02.036

741 Liew, P.Y., Lim, J.S., Wan Alwi, S.R., Abdul Manan, Z., Varbanov, P.S., Klemeš, J.J., 2014.
742 A Retrofit Framework for Total Site Heat Recovery Systems. Appl. Energy 135, 778–790.
743 https://doi.org/10.1016/j.apenergy.2014.03.090

744 Liew, P.Y., Wan Alwi, S.R., Varbanov, P.S., Manan, Z.A., Klemeš, J.J., 2013. Centralised
745 Utility System Planning for a Total Site Heat Integration Network. Comput. Chem. Eng.
746 57, 104–111. https://doi.org/10.1016/j.compchemeng.2013.02.007

747 LINDO Systems Inc., 2017. LINGO The Modelling Language and Optimizer. LINDO Systems
748 Inc., Chicago.

749 Lowe, E.A., Evans, L.K., 1995. Industrial Ecology and Industrial Ecosystems. J. Clean. Prod.
750 3, 47–53. https://doi.org/10.1016/0959-6526(95)00045-G

751 Malakrong, P., Wongsapai, W., Damrongsak, D., 2017. Analysis of Energy Utilization Index
752 in Thailand Sanitary Ceramics Sector. Energy Procedia 141, 170–174.
753 https://doi.org/10.1016/J.EGYPRO.2017.11.032

754 Ng, R.T.L., Hassim, M.H., Ng, D.K.S., Tan, R.R., El-Halwagi, M.M., 2014. Multi-Objective
755 Design of Industrial Symbiosis in Palm Oil Industry. Comput. Aided Chem. Eng. 34, 579–
756 584. https://doi.org/10.1016/B978-0-444-63433-7.50081-X

757 Ng, R.T.L., Ng, D.K.S., 2013. Systematic Approach for Synthesis of Integrated Palm Oil
758 Processing Complex. Part 1: Single Owner. Ind. Eng. Chem. Res. 52, 10206–10220.
759 https://doi.org/10.1021/ie302926q

760 Noureldin, M.M.B., El-Halwagi, M.M., 2015. Synthesis of C-H-O Symbiosis Networks.
761 AIChE J. 61, 1242–1262. https://doi.org/10.1002/aic.14714

762 Ohimain, E.I., Izah, S.C., 2017. A Review of Biogas Production from Palm Oil Mill Effluents
763 using Different Configurations of Bioreactors. Renew. Sustain. Energy Rev. 70, 242–253.
764 https://doi.org/10.1016/J.RSER.2016.11.221

765 Ponce-Ortega, J.M., Al-Thubaiti, M.M., El-Halwagi, M.M., 2012. Process Intensification: New
766 Understanding and Systematic Approach. Chem. Eng. Process. Process Intensif. 53, 63–
767 75. https://doi.org/10.1016/J.CEP.2011.12.010

768 Rubio-Castro, E., Ponce-Ortega, J.M., Nápoles-Rivera, F., El-Halwagi, M.M., Serna-González,
769 M., Jiménez-Gutiérrez, A., 2010. Water Integration of Eco-Industrial Parks using a Global

770 Optimization Approach. Ind. Eng. Chem. Res. 49, 9945–9960.
771 https://doi.org/10.1021/ie100762u

772 Rubio-Castro, E., Ponce-Ortega, J.M., Serna-González, M., El-Halwagi, M.M., 2012. Optimal
773 Reconfiguration of Multi-Plant Water Networks into an Eco-Industrial Park. Comput.
774 Chem. Eng. 44, 58–83. https://doi.org/10.1016/j.compchemeng.2012.05.004

775 Schneider, D.F., 1997. Debottlenecking Options and Optimization. Houston, Texas.

776 Sharifzadeh, M., 2013. Integration of Process Design and Control: A Review. Chem. Eng. Res.
777 Des. 91, 2515–2549. https://doi.org/10.1016/J.CHERD.2013.05.007

778 Siddiqi, M.Y., Glass, A.D.M., 1981. Utilization Index: A Modified Approach to the Estimation
779 and Comparison of Nutrient Utilization Efficiency in Plants. J. Plant Nutr. 4, 289–302.
780 https://doi.org/10.1080/01904168109362919

781 Song, R., Chang, C., Tang, Q., Wang, Y., Feng, X., El-Halwagi, M.M., 2017a. The
782 Implementation of Inter-Plant Heat Integration among Multiple Plants. Part II: The
783 Mathematical Model. Energy 135, 382–393.
784 https://doi.org/10.1016/j.energy.2017.06.136

785 Song, R., Tang, Q., Wang, Y., Feng, X., El-Halwagi, M.M., 2017b. The Implementation of
786 Inter-Plant Heat Integration among Multiple Plants. Part I: A Novel Screening Algorithm.
787 Energy 140, 1018–1029. https://doi.org/10.1016/j.energy.2017.09.039

788 Sustainable Energy Development Authority (SEDA) Malaysia, 2020. FiT Rates for Biogas (16
789 years from FiT Commencement Date) [WWW Document]. URL
790 http://www3.seda.gov.my/iframe/ (accessed 5.25.20).

791 Tan, R.R., Aviso, K.B., Cruz, J.B., Culaba, A.B., 2011. A Note on an Extended Fuzzy Bi-level
792 Optimisation Approach for Water Exchange in Eco-Industrial Parks with Hub Topology.
793 Process Saf. Environ. Prot. 89, 106–111. https://doi.org/10.1016/J.PSEP.2010.11.004

794 Tan, R.R., Lam, H.L., Kasivisvanathan, H., Ng, D.K.S., Foo, D.C.Y., Kamal, M., Hallaler, N.,
795 Klemeš, J.J., 2012. An Algebraic Approach to Identifying Bottlenecks in Linear Process
796 Models of Multifunctional Energy Systems. Theor. Found. Chem. Eng. 46, 642–650.
797 https://doi.org/10.1134/S004057951206022X

798 Ubando, A.T., Culaba, A.B., Aviso, K.B., Tan, R.R., Cuello, J.L., Ng, D.K.S., El-Halwagi,
799 M.M., 2016. Fuzzy Mixed Integer Non-Linear Programming Model for the Design of an
800 Algae-based Eco-Industrial Park with Prospective Selection of Support Tenants under
801 Product Price Variability. J. Clean. Prod. 136, 183–196.
802 https://doi.org/10.1016/j.jclepro.2016.04.143

803